Title

Vasoactive Intestinal Polypeptide (VIP) Regulates Metabolic Processes in Human and Murine Adipocytes by Modulating PPARγ Expression

Author

Luong, Leon

Publication Date

2017

UNIVERSITY OF CALIFORNIA

Los Angeles

Vasoactive Intestinal Polypeptide (VIP) Regulates Metabolic Processes in Human and Murine Adipocytes by Modulating PPARγ Expression

A thesis submitted in partial satisfaction of the requirements for the degree Master of Science in Physiological Science

by

Leon Luong

2017

ABSTRACT OF THE THESIS

Vasoactive Intestinal Polypeptide (VIP) Regulates
Metabolic Processes in Human and Murine Adipocytes
by Modulating PPARγ Expression

by

Leon Luong

Master of Science in Physiological Science
University of California, Los Angeles, 2017
Professor Joseph R. Pisegna, Co-Chair
Professor James G. Tidball, Co-Chair

Vasoactive intestinal peptide (VIP) is a neuropeptide expressed centrally in the hypothalamus and peripherally in the GI tract and adipose tissue. VIP and its VPAC receptors regulate body composition, as implicated by pathway-based, genome-wide association studies. We have previously shown that $VIP^{-/-}$ mice have lower fat mass and higher lean mass than their wild-type littermates. To elucidate the role of VIP in fat mass accumulation, $VIP^{-/-}$ mice were fed a 45% high-fat diet for 12 weeks. We determined that $VIP^{-/-}$ mice were resistant to weight gain and fat mass accumulation and had altered feeding behaviors and metabolic hormone levels. VIP antagonism of differentiating pre-adipocytes inhibited induction of adipocyte-related genes, such as PPARγ and C/EBP. Genetic association analyses using data from the METAbolic Syndrome in Men (METSIM) study showed a positive correlation between VIP, $VPAC_1R$ and key genetic

drivers of adipogenesis. These results implicate VIP's role in modulating fat accumulation.

The thesis of Leon Luong is approved.

Xia Yang

Joseph R. Pisegna, Committee Co-Chair

James G. Tidball, Committee Co-Chair

University of California, Los Angeles

2017

TABLE OF CONTENTS

CHAPTER 1: INTRODUCTION

Obesity is a major global health problem and the accumulation of adipose tissue has been associated with the development of type 2 diabetes, atherosclerosis, hyperlipidemia, chronic inflammation, and cancer. The molecular mechanism linking nutritional factors with hormonal regulation of adipocyte physiology is still unclear. Adipose tissue expansion involves cellular hypertrophy and hyperplasia. Adipogenesis, the process by which pre-adipocytes differentiate into adipocytes, occurs in several stages: mesenchymal precursor, committed pre-adipocytes, growth-arrested pre-adipocytes, mitotic clonal expansion, terminal differentiation and mature adipocyte. Sequential activation of transcription factors triggers adipogenesis. Transient expression of CCAAT/enhancer-binding protein-β (C/EBP-β) and -δ (C/EBP-δ) directly induces C/EBP-α and peroxisome proliferator-activated receptor-γ (PPARγ) expression. PPARγ then induces the expression of many downstream target genes like lipoprotein lipase (LPL), adipocyte protein 2 (aP2) and adiponectin (Rosen and MacDougald, 2006). A balance of local, adipogenic endocrine molecules regulate these mechanisms (MacDougald and Mandrup, 2002). Here, we demonstrate that Vasoactive Intestinal Peptide (VIP) regulates adipogenesis through these pathways.

VIP, a 28-amino acid neuropeptide, is highly expressed in central and peripheral nervous tissues and neurons (Lam, 1991; Hill et al., 1999; Dejda et al., 2005; Nussfdorfer and Malendowicz, 1998; Vosko et al., 2007). VIP acts as a neuromodulator, neurotransmitter, and neuroendocrine hormone through its three G-protein-coupled receptors: $VPAC_1R$, $VPAC_2R$, and PAC1 (Harmar et al., 2012). VIP is localized in the suprachiasmatic nucleus (SCN) of the hypothalamus (Usdin et al., 1994), where it synchronizes SCN neurons. SCN neurons ensure rhythmic clock gene expression, which is necessary towards maintaining a coherent circadian

rhythm under constant conditions (Harmar et al., 2002). Thusly, VIP and $VPAC_2R$ deficient mice exhibit: arrhythmic wheel running, desynchronized SCN neurons, and attenuated expression of PER1, PER2, and BMAL1 clock genes (Loh et al., 2011). In addition to regulating clock gene expression in the SCN and peripheral organs, VIP-$VPAC_2R$ interactions within the arcuate nucleus of the hypothalamus (ARC) regulate food intake and energy homeostasis (Berthoud 2002). Intracerebrovascular (ICV) and intraperitoneal (IP) injections of VIP decreased food intake in goldfish (Matsuda et al., 2005), chick (Tachibana et al., 2003), and rat (Olszewski et al., 2003) models. Moreover, VIP and $VPAC_2R$ knockout mice show disruptions in food intake and metabolic rhythms (Bechtold et al., 2008). Lastly, Hypothalamic VIP levels gradually increased in rats and decreased in chickens following a 36-hour fast (Jozsa et al., 2006), demonstrating that nutritional status affects hypothalamic VIP levels. Altogether, these studies implicate VIP's role in the hypothalamic control of food intake and energy homeostasis.

Besides regulating circadian rhythm and energy homeostasis, VIP's contribution to the regulation of adipogenesis is considered for the following reasons. First, pathway-based, genome-wide association analysis (GWAS) of 1,000 US Caucasians showed that the VIP pathway was most associated with fat mass and third most with BMI (Liu et al., 2010). Secondly, VIP and its receptors, $VPAC_1R$ and $VPAC_2R$, are necessary for growth, development, and metabolic regulation. For instance, $VPAC_1R^{-/-}$ mice exhibited growth retardation and metabolic rate increase (Ascinar et al., 2002), while $VPAC_2R^{-/-}$ mice showed insulin secretion impairment (Winzell et al., 2007). Thirdly, VIP-regulated clock genes, BMAL1 and PER2, have been implicated in adipogenesis and lipid metabolism. BMAL1 knockdown of NIH 3T3-L1 cells attenuated adipogenesis (Shimba et al., 2005) and $PER2^{-/-}$ mice displayed altered lipid metabolism (Grimaldi et al., 2010). Lastly, we previously published that standard diet (SD)-fed,

VIP-deficient mice had reduced body weight and fat mass and increased lean mass when compared to their WT counterparts. $VIP^{-/-}$ mice also showed altered feeding behaviors and abnormal plasma levels of adiponectin, α-ghrelin, GLP-1, leptin, PYY, and insulin (Vu et al., 2015).

In the current study, we demonstrate that $VIP^{-/-}$ mice are resistant to 45% HFD-induced fat mass accumulation and display disrupted feeding behaviors and metabolic hormone levels. VIP antagonism of differentiating NIH 3T3-L1 cells inhibited adipogenesis and the induction of adipocyte-related genes, such as PPARγ and C/EBP. Genetic association analyses using data from the METAbolic Syndrome in Men (METSIM) study showed a positive correlation between VIP, $VPAC_1R$ and key genetic drivers of adipogenesis. Our results support the hypothesis that VIP determines body composition by modulating the molecular pathways that promote adipogenesis.

CHAPTER 2: MATERIALS AND METHODS

Animals

Male and female VIP$^{-/-}$ mice (5-21 weeks of age, backcrossed >12 generations to C57BL/6J mice) were raised and genotyped as previously described (Colwell et al., 2003). Age-matched male and female WT littermates from the same colony were housed and fed *ad libitum* in a sterile animal facility, under controlled illumination (12:12-H light-dark cycle; lights from 06:00 to 18:00 hours) at the Veteran Affairs Greater Los Angeles Healthcare System animal facility. The Veterans Administration Institutional Animal Care and Use Committee dictated recommendations for animal use and welfare.

Body weight composition analysis

Mice were weaned at 3-4 weeks of age, group-housed four to a cage, and received water and standard rodent diet (Prolab RMH 2500; LabDiet, St. Louis, MO) *ad libitum*. During the experiment, mice were single-housed and fed either a SD (9 WT and 8 VIP$^{-/-}$ male mice; 8 WT and 11 VIP$^{-/-}$ female mice) or 45% HFD (14 WT and 11 VIP$^{-/-}$ male mice; 8 WT and 12 VIP$^{-/-}$ female mice). Body weight and body composition, as determined by nuclear magnetic resonance via an EchoMRI body composition analyzer (EchoMedical Systems, Houston, TX), was recorded every other week for 12 weeks. Body fat and lean mass changes were calculated as percent change from baseline. A two-way ANOVA was used to determine significance between the two-way interaction of study duration (12-weeks) versus weight, fat, and lean mass accumulation.

Determination of feeding behavior

BioDAQ (Research Diets, Inc., New Brunswick, NJ) episodic food intake monitor system was used to study feeding behavior as described previously (Stengel 2010). Male $VIP^{-/-}$ (n=16) and WT (n=16) mice were individually habituated for 7 days in separate BioDAQ cages and fed either a SD (8 WT and 8 $VIP^{-/-}$ male mice) or HFD (8 WT and 8 $VIP^{-/-}$ male mice). Food and water was given *ad libitum*. The BioDAQ system continuously monitored meal patterns of the mice using a cage-attached, low-spill food hopper on an electric balance. To ensure precise recording, we performed daily cage and food hopper inspections. Feeding intake data was measured over a 24-hour period and then separated into dark (18:00-06:00 hours) and light (06:00-18:00 hours) phases. Total food intake (grams) was recorded in 2-hour intervals. A "bout" is an individual feeding event calculated by dividing amount of food consumed over "meal" duration. A "meal" is a "bout" that lasts 5 minutes with a minimum of 0.02 g consumed. Bouts had to be more than 5 minutes apart to be considered a "meal." Analysis of meal parameters was calculated using BioDAQ Monitoring Software 2.2.02. Meal data was represented as: meal frequency, meal size (milligram), meal duration (minute), inter-meal interval, eating rate (meal size divided by duration of an analyzed period (12 hours)), and satiety ratio (average inter-meal interval divided by average meal size). Data was collected for two consecutive days and averaged.

Metabolic hormone measurements

At the end of the 12-week experiment, blood plasma was obtained from HFD-fed WT (n=12) and HFD-fed $VIP^{-/-}$ (n=9) male mice after an overnight fast (18:00-06:00 hours). Blood plasma was also collected during "postprandial conditions," which consisted of an overnight fast with a superseding refeeding period an hour before plasma collection. Protease inhibitors containing

DPPIV (Millipore; Billerica, MA), Roche Complete Protease Inhibitor Cocktail (Roche), Aprotinin (Fisher Scientific), and Roche Pefabloc SC (AEBSF) (Roche) was added to the collected plasma. Plasma was stored frozen at minus 80C until assayed. Plasma levels of active-ghrelin, GLP-1, glucagon, insulin, and peptide YY (PYY) were analyzed in duplicate using Milliplex MAP Mouse Metabolic Hormone Magnetic Bead Panel (Millipore, Billerica, MA). Hormone concentrations between groups were analyzed using a 2-way ANOVA.

Analysis of adipose tissue morphology

At the end of the experiment, animals were euthanized per recommendations of the Veterans Administration Institutional Animal Care and Use Committee (IACUC). Epididymal fat depots were then collected. WT HFD (n=9) and $VIP^{-/-}$ HFD (n=8) epididymal fat depots were fixed in 4% formaldehyde, embedded in paraffin wax, and sectioned (5 μm cuts). Adipose sections were stained with hematoxylin and eosin (H&E) and images were captured with bright-field microscopy at x200 magnification (Cardiff et al., 2014). White adipose tissue cellularity was analyzed by Adiposoft, an ImageJ plugin and open-source software (Galarraga et al., 2012). Adiposoft provided estimations of adipocyte diameter (μm). A one-way ANOVA was used to determine differences in epididymal fat morphology between genotypes and diets.

Cell culture

3T3-L1 cells were grown in DMEM supplemented with 10% calf serum, 100 U/ml penicillin, 100 mg/ml streptomycin, and in 8% CO2/ humidified atmosphere at 37°C. Adipogenic differentiation was induced 2-days post-confluence by incubating cells for 72 hours in DMEM containing: 10% fetal bovine serum (FBS), 500 μM IBMX, 0.25 μM dexamethasone, and 10 μg/

mL insulin. Experimental conditions included stimulation with 100 nm, 1 μM, or 10 μM of VIPHyb, a VIP antagonist (Li et al., 2012). Following 72 hours of differentiation, the cells from both control and experimental groups were maintained in medium supplemented with 10% FBS and insulin only. Medium was replaced daily at 16:00 hours. Cells were harvested at the following time points: day 0 (undifferentiated confluent cells), day 1 (first day of differentiation), day 3 (last day of differentiation), and day 5 (cells in medium supplemented with insulin only) for real-time PCR and Western Blot.

Oil-Red-O Staining

Oil-Red-O (ORO) staining of lipid vesicles allows verification of pre-adipocyte differentiation to adipocytes (Ramírez-Zacarías et al., 1992). ORO staining was implemented on day 9 of the differentiation protocol described above. Cells were rinsed with PBS and fixed with 4% paraformaldehyde for 15 min. Cells were washed 2 times with PBS and once with 60% isopropanol before incubation with ORO solution for 1 hour. Cells were then rinsed under running water for 1-2 minutes and photographed with a bright-field, light microscope under x200 magnification. To quantify the triglycerides content of the adipocytes, ORO was extracted with 100% isopropanol and absorbance was measured by spectrophotometry at 500 nm (Arsenijevic et al., 2013).

RNA Isolation

Cells were harvested by scrapping in 1 ml Qiazol Lysis Reagent (Qiagen, Valencia, CA, U.S.A.). RNA extraction was immediately carried out using Qiagen RNeasy Mini Kit (Qiagen,

Valencia, CA, U.S.A.) according to manufacturer's instructions. RNA concentration, purity, and integrity were assessed as previously described (Arsenijevic et al., 2012).

Primer Design, cDNA Synthesis and qPCR

Primer design, cDNA synthesis, and qPCR were performed as previously described (Arsenijevic et al., 2012).

Real-Time Quantitative PCR Analysis

RNA underwent reverse transcriptase (RT) reaction via Superscript first-strand synthesis kit (Invitrogen, Carlsbad, CA). One microgram of RT product was added in a reaction with SYBR premix Taq (Takara Bio, Shiga, Japan) for real-time PCR that was performed on the CFX96 Touch Real-Time PCR Detection System (Bio-Rad, Hercules, CA). The cycle of threshold, C(T), was determined as the fluorescent signal of 1 standard deviation over the background. The efficiency of each primer pair was measured by amplification of known amount of cDNA starting material (10pg – 10ng). PPARγ, C/EBPα, C/EBPβ, C/EBP*δ* and SIRT1 target primer pair amplifications were compared with the reference primer pair (GAPDH) amplification in the same experiment for each RT product tested. All reactions were carried out in triplicate. We ran 3 separate plates and averaged the results. The fold change of the target gene was calculated as previously shown (Schmittgen and Livak, 2008). Melting curves established the purity of the amplified band.

Protein Extraction and Western Blot Analysis

NIH 3T3-L1 cells from the different time points of differentiation were washed with calcium- and magnesium-free PBS and lysed in 1 ml of lysis buffer containing 50 mM Tris/ HCl (pH 7.5), 150 mM NaCl, 0.5% Nonidet P40, 50 mM NaF, 1 mM sodium orthovanadate, dithiothreitol, and a cocktail of protease inhibitors (Complete EDTA free, Roche). Whole cell lysates were used to perform SDS-polyacrylamide gel electrophoresis (SDS-PAGE; 12% polyacrylamide gels) in the presence of 5% β-mercaptoethanol. Proteins were transferred to a nitrocellulose membrane and immunolabeled using primary antibodies against: PPARγ, C/EBPα, C/EBPβ, C/EBP*δ*, and SIRT1 (Cell Signaling, Danvers, MA, U.S.A.). Secondary anti-rabbit antibodies (Cell Signaling, Danvers, MA, U.S.A.) and an ECL chemiluminescence detection kit (GE Healthcare Bio-Sciences, Marlborough, MA, U.S.A.) were used to detect bound primary antibodies. Ponceau staining (Cell Signaling, Danvers, MA, U.S.A.) was used to ensure equivalent protein concentrations in all lanes.

METSIM Data

A protocol of the detailed phenotyping, genotyping, and exome sequencing of the participants and the statistical methods used to correlate transcript or protein levels to one another have been previously described (Laakso et al., 2017). Gene-by-gene correlations were generated from the adipose expression arrays using mid-weight bicorrelations (bicor) coefficients and p-values adjusted for multiple testing from the R package WGNCA (Langfelder and Horvath, 2008). Heatmaps showing VIP and $VPAC_1R$ correlation across adipogenic markers was constructed from the bicor coefficient of those two genes in the METSIM population and the top 50 transcripts within the GO term for "fat cell differentiation" (*GO Slim and Subset Guide* 2017).

Data Analysis

All analyses were conducted using SAS 9.4 software (Cary, NC, SAS Institute). Figures were generated using Graphed Prism 6 Software (La Jolla, CA).

CHAPTER 3: RESULTS

VIP$^{-/-}$ mice are resistant to a 45% high fat diet (HFD)

We previously determined that VIP$^{-/-}$ mice fed a standard diet (SD), from 5 to 22 weeks of age, had significantly lower body weight and fat mass and higher lean mass than their age-matched WT counterparts (Vu et al., 2015). Since VIP$^{-/-}$ mice were significantly leaner than WT controls, we wanted to determine if the VIP$^{-/-}$ phenotype would be resistant to a 45% HFD. Mice were fed a HFD for 12 weeks. Body weight and percent fat and lean mass were measured bi-weekly using a whole-body composition EchoMRI analyzer. HFD-fed VIP$^{-/-}$ mice had significantly lower body weight and fat mass and higher lean mass than WT mice (Fig. 1A-C). The same trend was observed when female VIP$^{-/-}$ mice were compared to their WT counterparts (Fig. 1D-F).

Epididymal fat was extracted from male mice after the study and stained with H&E. ImageJ was used to quantify adipose tissue hypertrophy. HFD-fed VIP$^{-/-}$ mice had significantly less epididymal fat (Fig. 2A) and adipose tissue hypertrophy (Fig. 2B) than their WT littermates.

VIP$^{-/-}$ mice have dysregulated feeding behavior

Feeding behavior was recorded to determine whether the leaner phenotype observed in VIP$^{-/-}$ mice could be attributed to either an altered or reduced food intake. Previous studies determined that VIP$^{-/-}$ mice in constant darkness had circadian disruptions in wheel running behavior (Loh et al., 2014). A BioDAQ episodic food intake monitoring system was used to record 24-hour cumulative food intake (Fig. 3A). 24-hour cumulative food intake data was then further broken down into different meal parameters (Fig. 3C-G).

We previously demonstrated that SD-fed VIP$^{-/-}$ mice ate consistently throughout a 24-hour period, whereas WT mice primarily during the dark phase (18:00-06:00 hours) (Vu et al., 2015). In the current study, the same feeding trend was observed in HFD-fed VIP$^{-/-}$ mice (Fig. 3A). These findings were confirmed when cumulative food intake was further broken down into meal events such as: meal frequency, meal duration, meal size, percent time in meals, and eating rate (Fig. 3C-G). HFD-fed VIP$^{-/-}$ mice had a higher meal frequency during the light phase than WT mice (Fig. 3C). There were no differences in meal duration between WT and VIP$^{-/-}$ mice, with respect to either dark or light phase (Fig. 3D). VIP$^{-/-}$ mice had a higher meal size in the light phase (Fig. 3E). Percent time in meals was significantly reduced for VIP$^{-/-}$ mice during the dark phase (Fig. 3F). Finally, VIP$^{-/-}$ mice had a significantly higher eating rate than WT mice during the light phase (Fig. 3G). Despite differences in feeding behavior, VIP$^{-/-}$ and WT mice consumed equal amounts of food within a 24-hour period (Fig. 3B).

These results demonstrate that VIP$^{-/-}$ mice have altered feeding behaviors but similar cumulative food intake when compared to WT mice. Furthermore, previous calorimetric recordings showed no differences in basal energy expenditure between VIP$^{-/-}$ and WT mice (Bechtold et al., 2008). Collectively, analyses of total food intake and energy expenditure did not identify a specific cause for the leaner phenotype of the VIP$^{-/-}$ mice.

VIP$^{-/-}$ mice have a dysregulated metabolic hormone profile

Therefore, the decreased adiposity observed in VIP$^{-/-}$ mice may be due to VIP's role in modulating the release of metabolic hormones in the arcuate nucleus of the hypothalamus (ARC) and energy-sensing organs in the periphery. Metabolic hormones released in the ARC and peripheral organs then modulate energy homeostasis and body composition (Williams et al.,

2000). VIP has been implicated in regulating GI epithelial cell secretion and release of pituitary and pancreatic hormones (Sherwood et al., 2000). Additionally, the obesogenic effects of a HFD can be attributed to the dysregulation of metabolic hormones. HFDs have been shown to increase the number of ghrelin precursor-expressing cells and the affinity of ghrelin-reactive IgG, which protects active-ghrelin from degradation (Francois et al., 2016). Mice fed a HFD developed hyperleptinemia and hyperinsulinemia (Chakraborty et al., 2016) and have a higher density of GLP-1 and PYY-secreting L-cells (Aranias et al., 2015). Increased GLP-1 secretion is an adaptive response of the intestine to balance HFD-induced insulin resistance (Aranias et al., 2015).

Previous studies have shown that $VIP^{-/-}$ mice have elevated plasma levels of glucose, insulin, and leptin concentrations and decreased plasma levels of adiponectin (Martin et al., 2010; Vu et al., 2015). VIP signaling is necessary for regulating insulin and glucagon secretion since $VPAC_2R^{-/-}$ mice developed glucose intolerance and impaired insulin secretion (Moody et al., 2011) and $VPAC_1R^{-/-}$ mice had increased insulin sensitivity and reduced serum leptin levels (Harmar et al., 2012). We wanted to determine whether VIP deficiency downregulates the expression of metabolic hormones associated with HFD-induced lipogenesis and adipogenesis. Fasting and postprandial plasma concentrations of active-Ghrelin, glucagon-like peptide 1 (GLP-1), glucagon, insulin, and PYY were measured in HFD-fed mice using a Metabolism Multiplex Assay. HFD-fed $VIP^{-/-}$ mice had lower fasting plasma concentrations of active-ghrelin (Fig. 4A) and glucagon (Fig. 4C) and lower postprandial concentrations of GLP-1 (Fig. 4B), glucagon (Fig. 4C), insulin (Fig. 4D), and peptide YY (PYY) (Fig. 4E) when compared to WT littermates.

VIP, via $VPAC_2R$, has been shown to stimulate insulin secretion in a glucose-dependent manner and also glucagon secretion in response to hypoglycemia (Winzell and Ahrén, 2007).

However, the mechanisms by which VIP modulates ghrelin, GLP-1, and PYY secretion have yet to be elucidated. These hormones are secreted in the GI tract before binding to their respective receptors in the ARC. VIPergic neurons are densely localized in both the GI tract and ARC, thereby potentially modulating ghrelin, GLP-1, and PYY release. Ultimately, VIP is necessary for the robust expression of adipogenic hormones and that elevated concentrations of these adipogenic hormones are potent signals for adipose tissue expansion.

VIP is required for adipogenesis in NIH 3T3-L1 cells

VIP deficiency dampened plasma concentrations of adipogenic hormones, thereby indirectly attenuating lipogenesis and adipogenesis. We then wanted to determine whether VIP is directly involved in the induction of pre-adipocyte differentiation. To accomplish this, we utilized the NIH 3T3-L1 cells, a prominent cell line used in the study of adipogenesis (Shimba et al., 2005). We first verified the presence of $VPAC_1R$ and $VPAC_2R$ on NIH 3T3-L1 cells using qPCR (Fig. 5A). These results were corroborated by previous studies utilizing the 3T3-L1 cell line (Alexander et al., 1995; Akesson et al., 2005). VIP also dose-dependently increased cAMP response in 3T3-L1 cells, as determined by ELISA (Fig. 5B). Adipocyte differentiation was induced, 48-hours post-confluence, by incubating the cells for 72 hours in DMEM containing: 10% fetal bovine serum (FBS), IBMX, dexamethasone, and insulin. To verify VIP's involvement in adipogenesis, differentiating 3T3-L1 cells were co-treated with varying dosages of VIPHyb (100 nm, 1 μM, or 10 μM), a VIP receptor antagonist (Li et al., 2013). Following 72 hours of differentiation, the cells were maintained in medium supplemented with 10% FBS and insulin only. The degree of differentiation of VIPHyb-stimulated cells was compared to unstimulated, differentiating or non-differentiating controls. VIPHyb dose-dependently inhibited

lipid accumulation, as determined by oil red staining and spectrophotometry (Fig. 5C). VIPHyb administered at 10 μM was most effective at attenuating adipogenesis (Fig. 5C).

VIP regulates gene expression of lipogenesis-related factors in NIH 3T3-L1 adipocytes

To elucidate the role of VIP in the cellular accumulation of lipids, differentiating 3T3-L1 cells were simultaneously treated with 10 μM of VIPHyb and harvested on days 1, 3, and 5 of differentiation for qRT-PCR and Western Blotting (Fig. 6). Expression of adipogenic transcription factors: C/EBPα, C/EBPβ, C/EBPδ, and PPARγ was determined. The activation of these adipogenic transcription factors is necessary for pre-adipocyte differentiation (Rosen and MacDougald, 2006). During differentiation, there is a burst of C/EBPβ and C/EBPδ activation, which triggers PPARγ induction. PPARγ then initiates C/EBPα expression. Finally, a positive feedback loop between PPARγ and C/EBPα is formed, thus activating the full program of adipogenesis (Rosen and MacDougald, 2006). Studies have described PPARγ as a potent inducer of adipogenesis and fatty acid storage (Farmer, 2005), therefore making it a therapeutic target for many anti-obesogenic drugs (Feng et al., 2016).

Our results show that VIP antagonism inhibits mRNA expression of key adipogenic transcription factors. For instance, C/EBPβ (Fig. 6C) and C/EBPδ (Fig. 6D) mRNA concentrations were downregulated 24 hours after VIPHyb stimulation. Additionally, PPARγ (Fig. 6A) and C/EBPα (Fig. 6B) transcript levels were downregulated on Day 3. In VIPHyb-treated NIH 3T3-L1 cells, protein analyses revealed that C/EBPβ levels were attenuated on Day 1 of VIPHyb treatment, whereas PPARγ and C/EBPα levels were reduced on Days 1 and 3 (Fig. 6F). Transcript and protein levels of SIRT1, a PPARγ co-repressor, were elevated throughout the

experiment (Fig. 6E-F). These findings show that blocking VIP receptors resulted in the transcriptional and translational suppression of key adipogenic factors.

VIP expression is positively associated with the expression of adipogenic factors in the humans

Since VIP antagonism down-regulated the expression of key adipogenic transcription factors, our aim was to determine if these relationships persisted in healthy human populations. Therefore, we interrogated adipose tissue expression arrays from the METabolic Syndrome in Men (METSIM) study for correlations between VIP, $VPAC_1R$, and key genetic drivers of adipogenesis. The METSIM study consists of cross-sectional and follow-up study designs that include deep phenotyping of 10,197 healthy Finnish men, aged from 45-73 years, and extensive DNA- and RNA-based genetic studies (Laakso et al., 2016). Subcutaneous adipose tissue samples were collected from 770 participants and subjected to global expression arrays (Laakso et al., 2016). Gene-by-gene correlations were generated from the adipose expression arrays using mid-weight bicorrelations (bicor) coefficients and p-values adjusted for multiple testing from the R package WGNCA. Heatmaps showing VIP and VPAC1R correlation across adipogenic markers were constructed from the bicor coefficient of these two genes in the METSIM population and the top 50 transcripts within the GO term for "fat cell differentiation (Fig. 7A)." Therefore, VIP is not only modulating transcriptional activators of PPARγ, but a whole host of other adipogenic pathways as well.

Scatterplots of the most statistically significant gene versus gene correlations demonstrate a positive association between VIP expression and integral genetic drivers of adipogenesis: PPARγ (Fig. 7B), C/EBPα (Fig. 7C), C/EBPγ (Fig. 7D), and LXRα (Fig. 7E). No significant

associations between VIP and transcript expression levels of C/EBPβ, C/EBPδ, and SIRT1 were identified. This observed inconsistency may be due to variation between study designs, and/ or population- or species-specific variations in gene expression. Similar inconsistencies are also commonly observed between animal studies and population-based associations, despite sufficiently controlled study designs (Laakso et al., 2017). While the METSIM study allows us to observe relationships within a genetically diverse population, it is also restricted to middle-aged Finnish men. Nevertheless, these results reveal a novel relationship between VIP and pro-adipogenic machinery.

CHAPTER 4: DISCUSSION

In this study, we demonstrated that VIP signaling is required for adipocyte differentiation and fat mass expansion. HFD-fed $VIP^{-/-}$ mice gained significantly less body weight and fat mass and retained more lean mass than their WT littermates (Fig. 1). Histological sections of epididymal fat revealed dramatically lower hypertrophy and lipid accumulation in HFD-fed $VIP^{-/-}$ mice (Fig. 2). HFD-fed $VIP^{-/-}$ mice displayed altered feeding behaviors, although similar cumulative food intake when compared to WT controls (Fig. 3). Therefore, the leaner body composition of $VIP^{-/-}$ mice is likely attributed to ulterior mechanisms and not caloric intake. Since VIP has been implicated in the regulation of GI epithelial cell secretion and release of pituitary and pancreatic hormones (Sherwood et al., 2000), we speculated that VIP deficiency could alter metabolic hormone secretions. In conjunction with this hypothesis, we found lower plasma concentrations of active-ghrelin (Fig. 4A), GLP-1 (Fig. 4B), glucagon (Fig. 4C), insulin (Fig. 4D), and peptide YY (PYY) (Fig. 4E) in HFD-fed $VIP^{-/-}$ mice.

Elevated levels of these hormones, in the context of excess caloric intake, have been shown to stimulate lipogenesis and adipogenesis (Larsson and Ahrén, 2000; Liu et al., 2016; Sangiao-Alvarellos et al. 2009; Viscarra et al., 2017; Shi et al., 2012). For instance, chronic administration of ghrelin, an orexigenic hormone released by the gastric P/ D1 cells, promoted lipogenesis and weight gain in mice without overfeeding (Sangiao-Alvarellos et al. 2009; Theander-Carrillo et al., 2006). Ghrelin directly affected energy partitioning, causing carbohydrates to be consumed over fat as a major fuel source (Longo et al., 2008). Similarly, *in vivo* and *in vitro* studies revealed that insulin stimulated lipogenesis and adipogenesis, while inhibiting lipolysis (Kahn and Flier, 2000; Viscarra et al., 2017). Insulin is produced by pancreatic β-cells and promotes glucose absorption into fat, liver, and skeletal muscle cells.

Prolonged hyperinsulinemia induced adipogenesis via sequential activation of adipogenic transcription factors like C/EBPα, C/EBPβ, and PPARγ (Klemm et al., 2001). In adipocytes, insulin promoted lipogenesis through glucose and lipoprotein-derived fatty acids uptake (Longo et al., 2008). Glucagon, which is produced by pancreatic α-cells, is released during hypoglycemia to stimulate glycogenolysis and gluconeogenesis in the liver and raise blood glucose (Larsson and Ahrén, 2000). However, inappropriately elevated glucagon levels were responsible for increased hepatic glucose production in type 2 diabetes, resulting in impaired glucose tolerance (Larsson and Ahrén, 2000). Deletion of the glucagon receptor gene yielded mice resistant to DIO (Vuguin et al., 2011). Furthermore, GLP-1, via the Wnt4/ β-catenin pathway, dose-dependently elevated transcript and protein expression of free fatty acid-binding protein 4 (aP2), PPARγ, C/EBPα, and lipoprotein lipase (LPL) in differentiating 3T3-L1 cells (Liu et al., 2016). Elevation of these adipocyte marker genes resulted in increased adipocyte differentiation and lipid accumulation (Liu 2016; Yang 2013). GLP-1 is secreted by L-cells in the small intestine in response to fat and carbohydrates ingestion to enhance glucose-dependent, insulin secretion (Liu et al., 2016). PYY, co-released with GLP-1 from enteroendocrine L-cells in response to a meal, acted on Y2 receptors in the ARC and on vagal afferents to increase satiety, therefore, making PYY essential in postprandial fuel assimilation (Shi et al., 2012). Transgenic mice overexpressing PYY exhibited an increased respiratory exchange ratio, corresponding to decreased lipid oxidation and increased lipogenesis (Zhang et al., 2012). Altogether, these studies and our results indicate a crucial role for VIP in the modulation of metabolic hormone secretions. The absence of VIP lead to abrogated release of these adipogenic hormones, thereby protecting $VIP^{-/-}$ mice from DIO.

VIP can also directly influence adipocyte metabolism via $VPAC_1R$ and $VPAC_2R$ (Fig. 5A-B). $VPAC_1R$ and $VPAC_2R$ deficient mice had dramatically lower body weights along with reduced fat mass (Ascinar et al., 2002; Fabricius et al., 2011). We showed that VIP antagonism reduced lipid accumulation in NIH 3T3-L1 pre-adipocytes (Fig. 5) and attenuated expression of several lipid metabolism-related factors (Fig. 6).

In particular, transcript and protein levels of C/EBPα, C/EBPβ, C/EBPδ, and PPARγ were down-regulated in differentiating 3T3-L1 cells treated with VIPHyb (Fig. 6). PPARγ is considered the principal regulator of adipogenesis. *In vitro* studies demonstrated that ectopic PPARγ expression was sufficient to cause non-precursor cells (fibroblasts and myocytes) to differentiate into adipocytes (Hu et al., 1995; Tontonoz et al., 1994). Mice with adipocyte-specific deletion of PPARγ exhibited insulin resistance and decreased adipose tissue mass (He et al., 2003). Therefore, mitigating PPARγ expression is a putative mechanism by which VIPHyb inhibits adipocyte maturation.

The majority of transcriptional repressors and activators known to modulate adipogenesis act through the regulation of PPARγ expression. We report upregulated levels of SIRT1, a co-repressor of PPARγ expression (Picard et al., 2004) (Fig. 6E). SIRT1 serves as a nuclear metabolic sensor that directly couples cellular metabolic status (via NAD+ levels) to chromatin structure, as well as, gene expression regulation through the deacetylation of histones, transcription factors, and transcription co-factors (Li 2013). Similar to VIP, SIRT1 is expressed on POMC and AgRP neurons of the ARC and serves to interpret adiposity and nutrient-related inputs. In mice, SIRT1 deletion in POMC neurons reduced leptin signaling and energy expenditure, ultimately sensitizing the mice to DIO (Ramadori et al., 2010). Also, SIRT1 suppression of PPARγ resulted in increased lipolysis, fatty acid oxidation, and fat loss in

differentiated adipocytes (Gehart-Hines et al., 2007; Yu et al., 2004; Zhou et al., 2016). Hence, VIPHyb-induced SIRT1 upregulation suppresses PPARγ and inhibits adipogenesis. However, the mechanism by which VIP regulates SIRT1 expression requires further elucidation.

In addition to regulating transcriptional activators of PPARγ, VIP also influences an assortment of transcripts implicated in fat cell differentiation, as signified by the METSIM study (Fig. 7A). Among the most notable associations is the correlation between VIP and C/EBPγ (Fig. 7D). C/EBPγ and C/EBPδ protein levels accumulate within the first hours of differentiation to stimulate expression of C/EBPα and PPARγ (Rosen and MacDougald, 2006). C/EBPα and PPARγ, master regulators of adipogenesis, were both also positively correlated to VIP transcript expression (Fig. 7B-C). Additionally, the METSIM study showed a significantly positive association between VIP and LXRα (Fig. 7E). The LXRα promoter is under the regulation of PPARγ and C/EBPα/ -β/ -δ. LXRs regulate enzymes involved in cholesterol degradation, reversing transport of cholesterol from peripheral cells, cholesterol uptake and lipogenesis (Steffensen et al., 2002). LXRα acts on downstream gene targets SREBP-1c (Repa et al., 2000) and acetyl CoA carboxylase (ACC) to activate fatty acid biosynthesis, regulate sterol metabolism, and stimulate lipid metabolism and uptake (Zhang et al., 2001). These studies demonstrate that in Finnish subjects, elevated VIP expression correspond to an upregulation of transcriptional activators that either facilitate fat cell differentiation or stimulate PPARγ expression.

We conclude that VIP utilizes a two-pronged approach to promote lipogenesis and adipogenesis during excess caloric intake. (1) VIP, released in the GI tract and ARC, may elicit robust metabolic hormone secretions necessary in the induction of adipogenesis. (2) VIP directly targets VPAC receptors on adipose tissue to upregulate adipogenic transcription factors and

activators of PPARγ, as shown by qRT-PCR, Western blotting, and METSIM studies. Regulation of the adipogenic machinery is integral in reversing obesity since adipogenesis is the precursor to adipose tissue hypertrophy. VIP's involvement in body composition, appetite, and adipogenesis makes it a novel target for the development of future therapeutic agents against obesity.

FIGURES

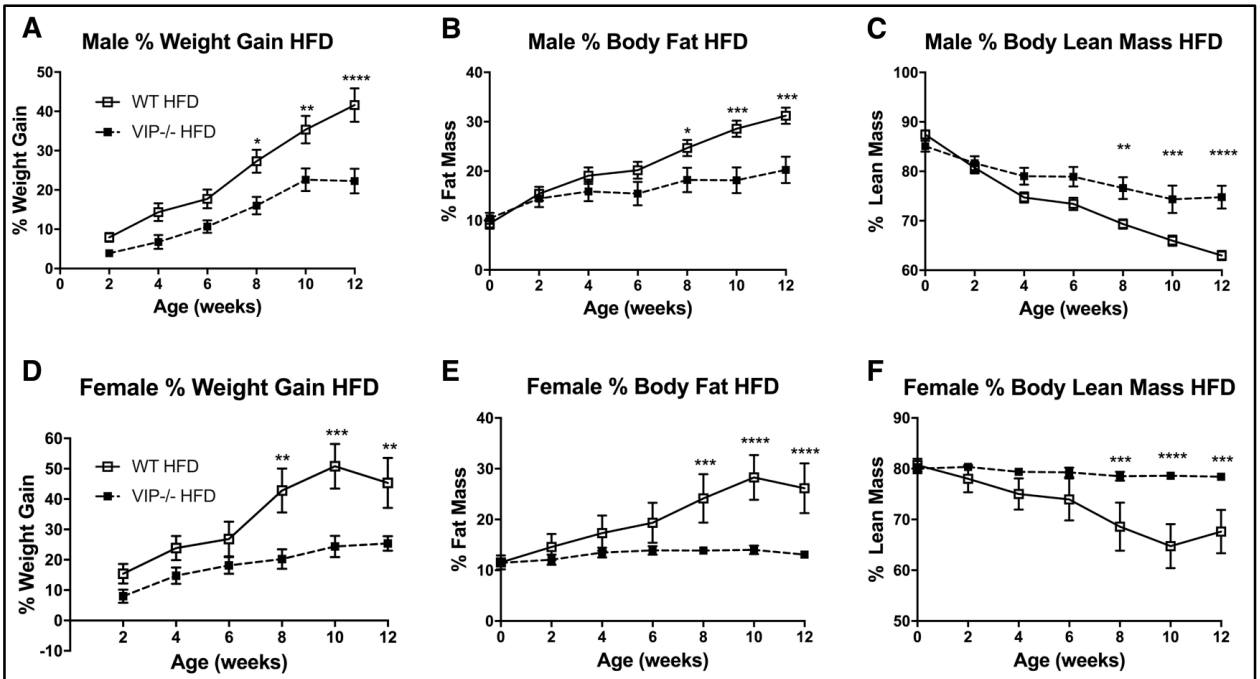

Figure 1. Vasoactive Intestinal Peptide ($VIP^{-/-}$) mice are resistant to a 45% high fat diet (HFD)

(A-F) Male and female WT or $VIP^{-/-}$ mice were fed a HFD for 12 weeks. Percent fat and lean mass were recorded using an EchoMRI body composition analyzer bi-weekly. (A-C) Male and (D-F) female $VIP^{-/-}$ HFD-fed mice had significantly lower body weight and fat mass and higher lean mass than their WT HFD-fed counterparts from weeks 8 to 12. Data are represented as mean ± SEM.

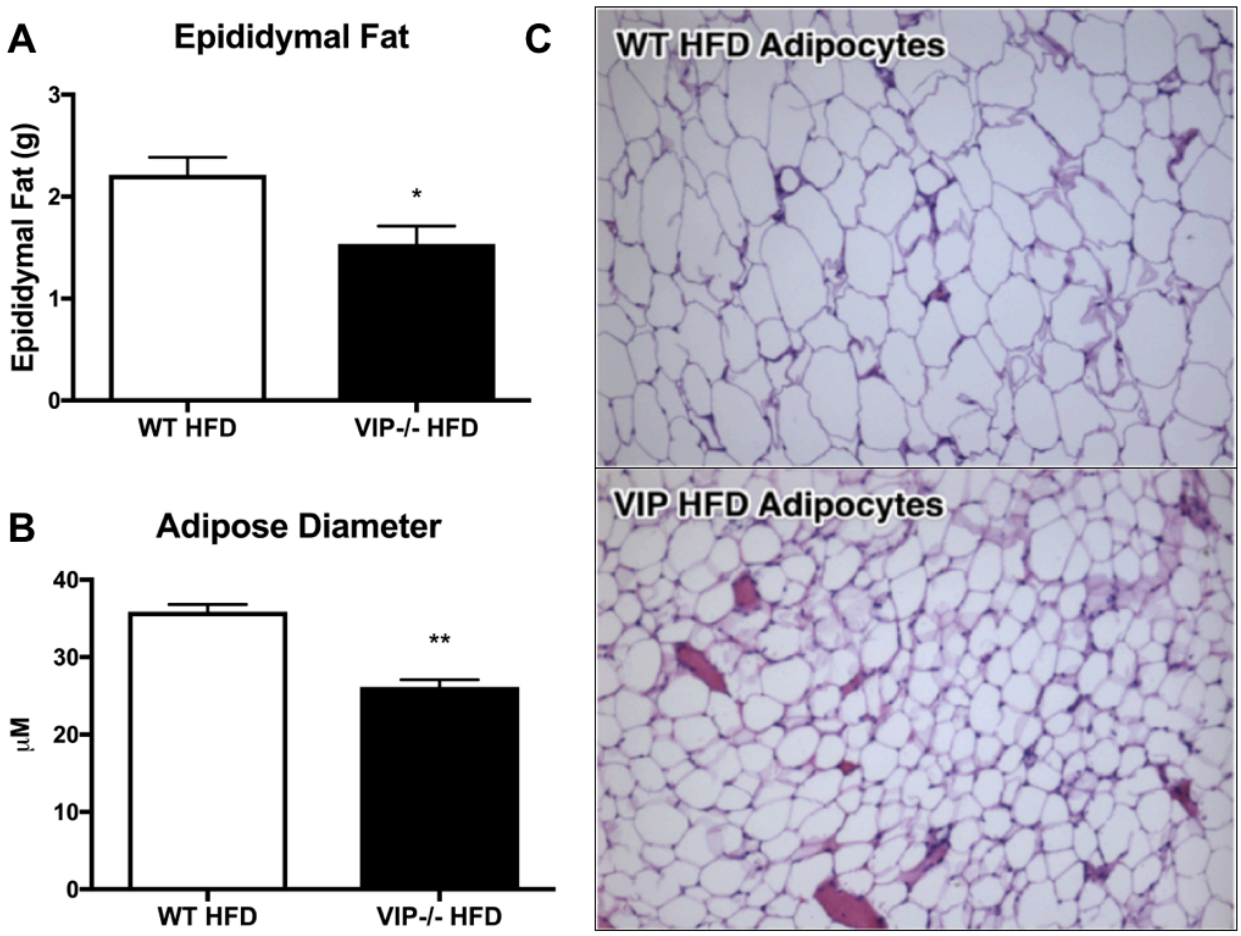

Figure 2. VIP$^{-/-}$ mice have reduced adipose tissue hypertrophy on a HFD
Adipose sections were stained with hematoxylin and eosin (H&E) and images were captured with bright-field microscopy at x200 magnification. Images were analyzed by Adiposoft, an ImageJ plug-in used to determine adipose tissue cellularity in histologic sections. HFD-fed VIP$^{-/-}$ mice had significantly reduced (A) epididymal fat and (B) adipose tissue diameters. (C) H&E stained epididymal sections from HFD-fed WT and VIP$^{-/-}$ mice.

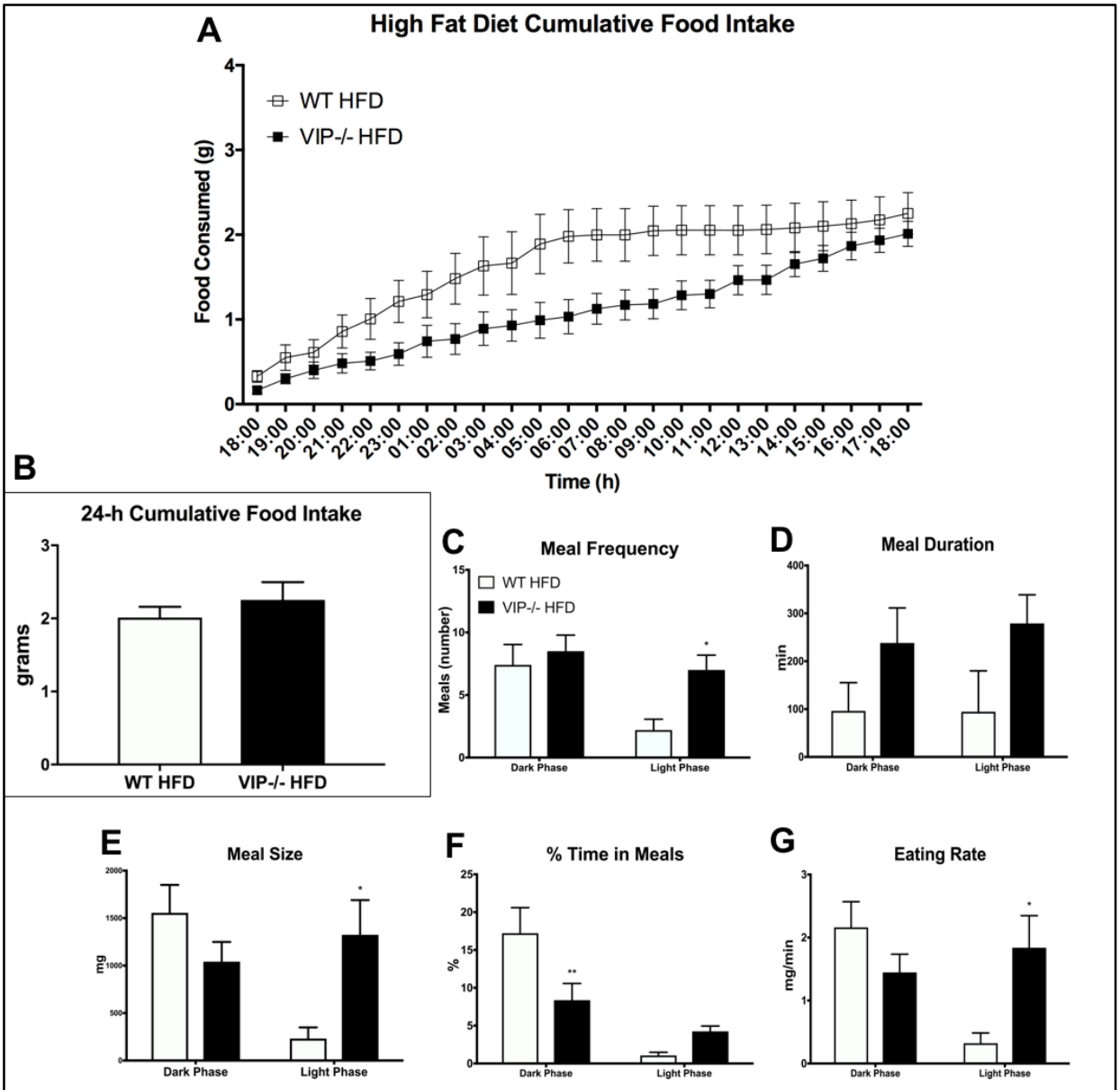

Figure 3. VIP$^{-/-}$ mice have dysregulated feeding behaviors
(A) 24-hour cumulative food intake data of male, HFD-fed WT and VIP$^{-/-}$ mice were recorded using a BioDAQ episodic food intake monitoring system. Data were collected over 2 days and averaged. Recordings revealed that WT mice ate solely during the dark phase (18:00-06:00 hours), whereas VIP$^{-/-}$ mice ate consistently throughout a 24-hour period. (B) Cumulatively, WT and VIP$^{-/-}$ mice ate similar amounts of food over a 24-hour period. (C) HFD-fed VIP-/- mice had a higher meal frequency during the light phase than WT mice. (D) There were no differences in meal duration between WT and VIP-/- mice, with respect to either dark or light phase. (E) VIP-/- mice had a higher meal size in the light phase. (F) Percent time in meals was significantly reduced for VIP-/- mice during the dark phase. (G) Finally, VIP-/- mice had a significantly higher eating rate than WT mice during the light phase. Data are represented as mean ± SEM.

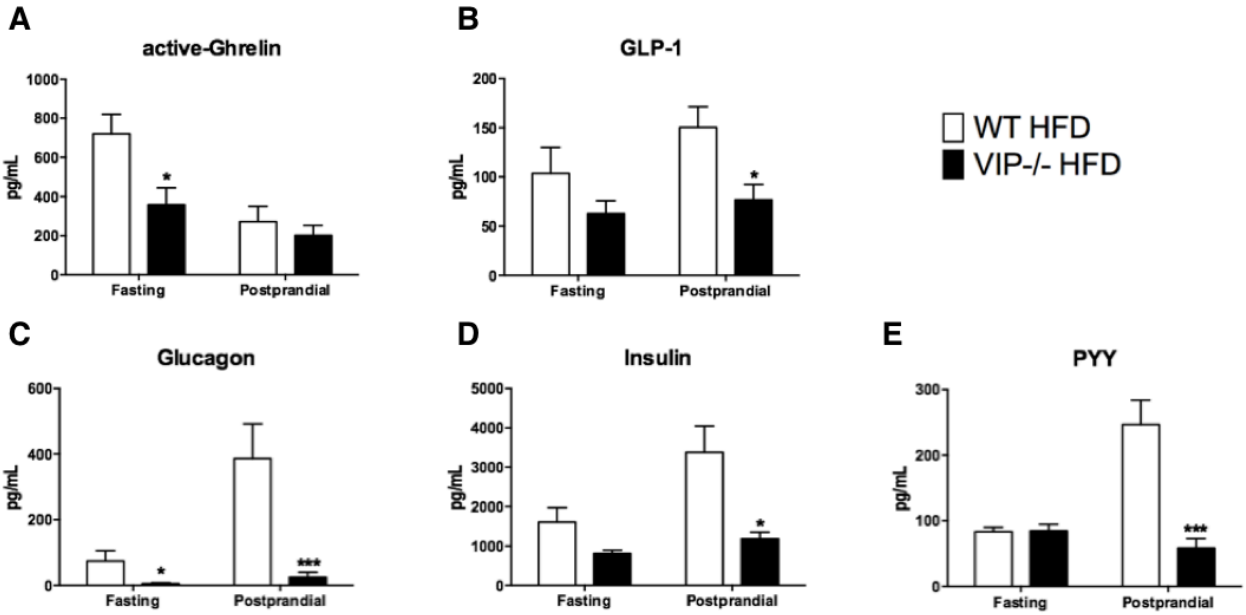

Figure 4. VIP$^{-/-}$ mice have dysregulated metabolic hormones

(A-E) Fasting conditions were established with an overnight fast (18:00-06:00 hours). Postprandial conditions were established with an overnight fast and a refeed period an hour before plasma collection. Metabolic hormone concentrations (pg/mL) were measured using Milliplex MAP Mouse Metabolic Hormone Magnetic Bead Panel.

(A) VIP-/- HFD-fed mice had significantly decreased fasting active-Ghrelin.

(B) GLP-1 was significantly reduced in VIP-/- HFD-fed under postprandial conditions.

(C) VIP-/- HFD-fed mice had reduced glucagon concentrations during fasting and postprandial conditions.

(D) Insulin levels were lower during postprandial conditions for VIP-/- HFD-fed mice.

(E) PYY was significantly lower in VIP-/- HFD-fed mice but only under postprandial conditions.

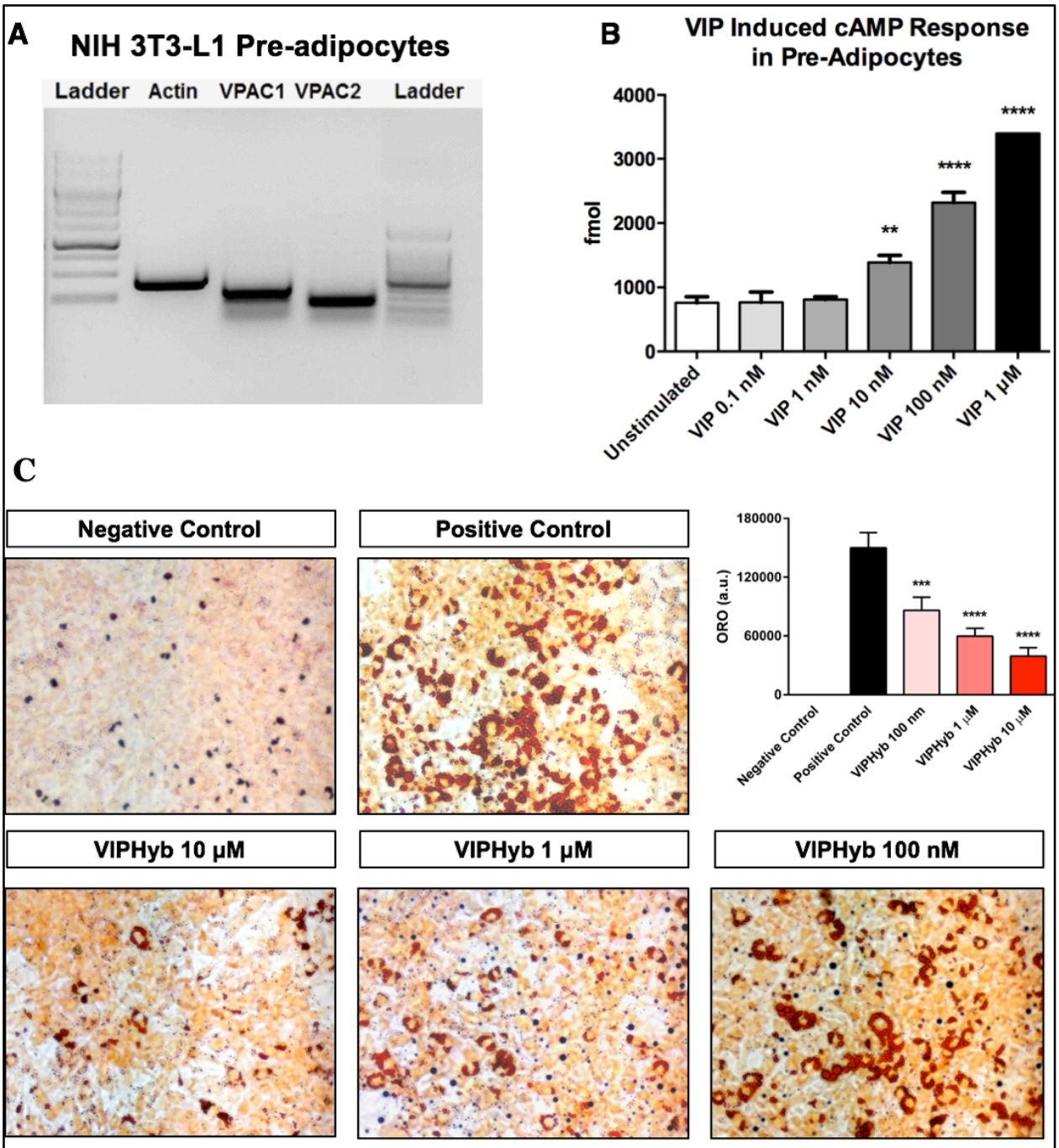

Figure 5. VIP is Required for Adipogenesis in NIH 3T3-L1 Cells
(A) The presence of VPAC1R and VPAC2R on 3T3-L1 cells was verified using qPCR. (B) VIP also dose-dependently increased cAMP response in 3T3-L1 cells, as determined by ELISA. (C) Differentiating 3T3-L1 cells were stimulated with varying doses of VIPHyb (100 nm, 1 µM, or 10 µM) for 72 hours. All doses of VIPHyb, successful mitigated pre-adipocyte differentiation, with 10 µM of VIPHyb being the most potent dose. Oil-Red-O staining and spectrophotometry at 500 nm was used to verify pre-adipocyte maturation. Data are represented as mean ± SEM.

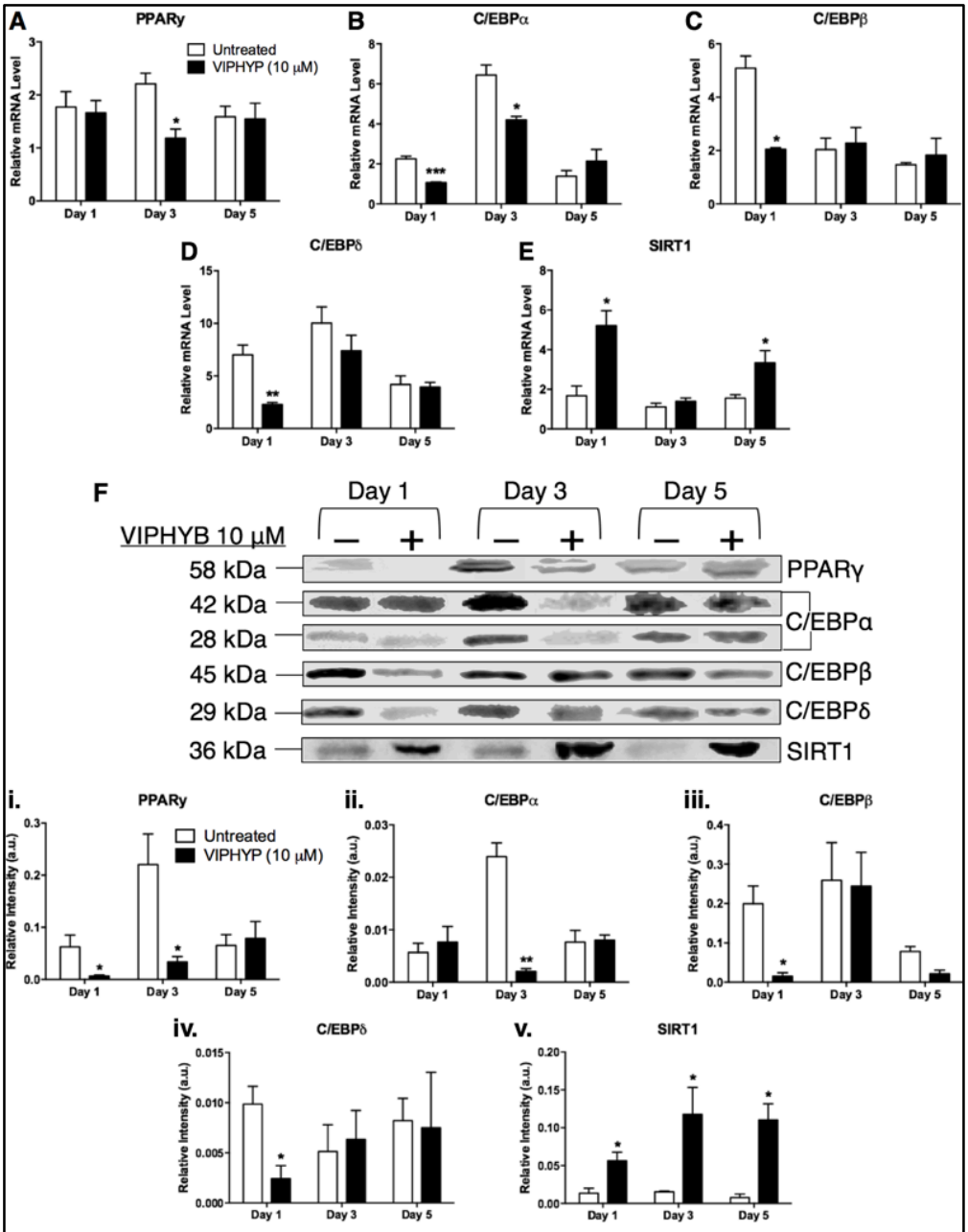

Figure 6. VIP Regulates Gene Expression of Lipogenesis-Related Factors in NIH 3T3-L1 Adipocytes

(A-E) Differentiating 3T3-L1 cells, treated with or without VIPHyb, were harvested for RT-PCR on: day 0 (undifferentiated confluent cells), day 1 (first day of differentiation), day 3 (last day of differentiation), and day 5 (cells in medium supplemented with insulin only). VIPHyb-treated cells had: (A) reduced PPARγ mRNA expression on day 3; (B) reduced C/EBPα mRNA expression on days 1 and 3; and reduced (C) C/EBPβ and (D) C/EBP*δ* mRNA expression on day 1. (E) SIRT1 expression was significantly higher in treated cells on days 1 and 5. (H) Protein expression was analyzed via Western Blot. Ponceau staining was used to verify uniform protein levels. In VIPHyb-treated cells, (H*i*) PPARγ protein expression was reduced on days 1 and 3 and (H*ii*) C/EBPα expression was reduced on day 3. VIPHyb-treated cells had reduced (H*iii*) C/EBPβ and (H*iv*) C/EBP*δ* protein levels on day 1. (H*v*) SIRT1 protein expression was upregulated throughout days 1 to 5 in VIPHyb-treated cells. Data are represented as mean ± SEM.

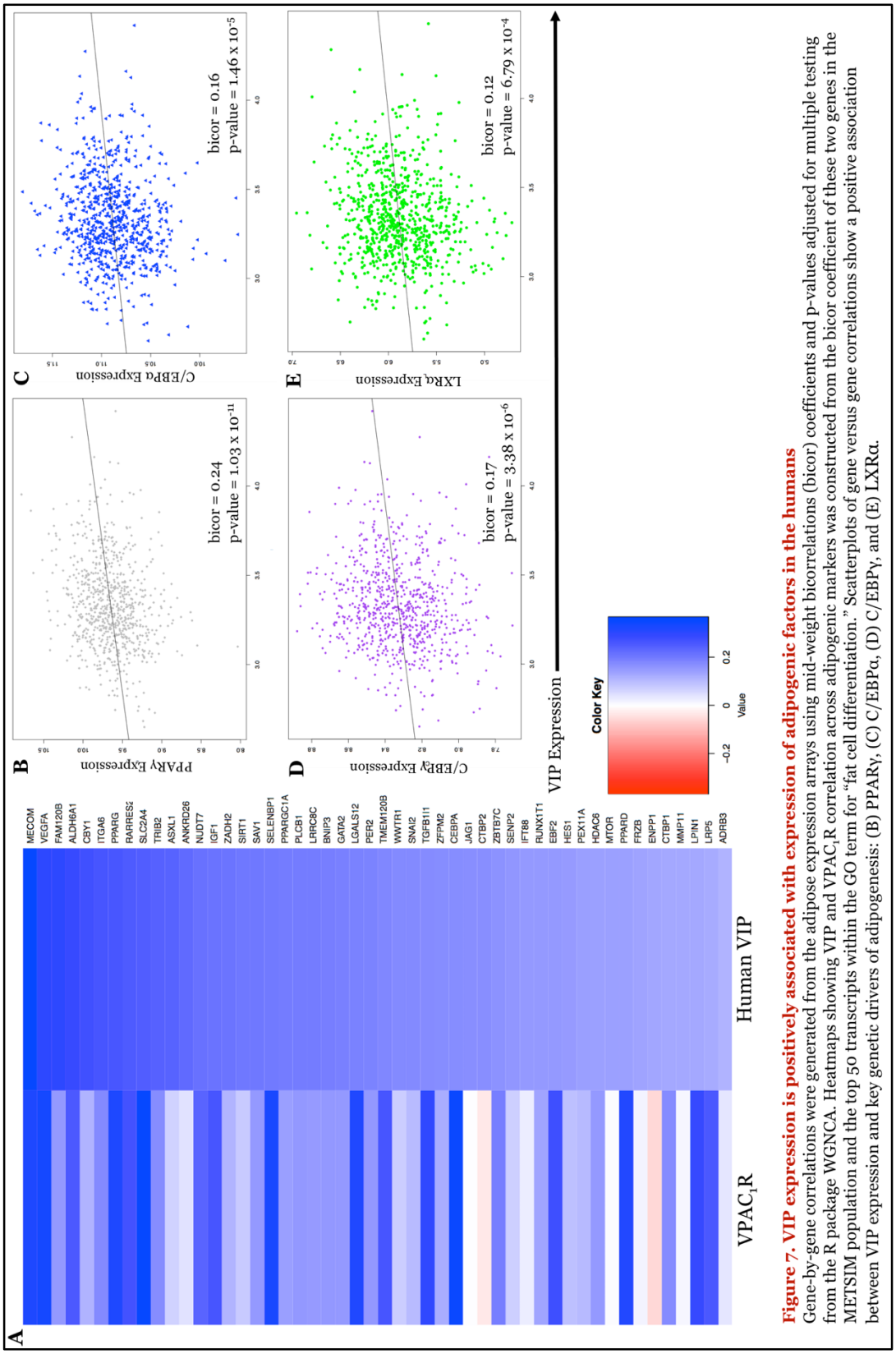

Figure 7. VIP expression is positively associated with expression of adipogenic factors in the humans
Gene-by-gene correlations were generated from the adipose expression arrays using mid-weight bicorrelations (bicor) coefficients and p-values adjusted for multiple testing from the R package WGNCA. Heatmaps showing VIP and $VPAC_1R$ correlation across adipogenic markers was constructed from the bicor coefficient of these two genes in the METSIM population and the top 50 transcripts within the GO term for "fat cell differentiation." Scatterplots of gene versus gene correlations show a positive association between VIP expression and key genetic drivers of adipogenesis: (B) PPARγ, (C) C/EBPα, (D) C/EBPγ, and (E) LXRα.

REFERENCES

1. Akesson, L., Ahrén, B., Edgren, G. and Degerman, E. (2005). VPAC2-R Mediates the Lipolytic Effects of Pituitary Adenylate Cyclase-Activating Polypeptide/Vasoactive Intestinal Polypeptide in Primary Rat Adipocytes. Endocrinology, 146(2), pp.744-750.
2. Alexander, LD., Evans, K., Sander, LD. (1995). A possible involvement of VIP in feeding-induced secretion of ACTH and corticosterone in the rat. Physiol Behav, 58(2), pp.409–413.
3. Aranias, T., Grosfeld, A., Poitou, C., Omar, A., Le Gall, M., Miquel, S., Garbin, K., Ribeiro, A., Bouillot, J., Bado, A., et al. (2015). Lipid-rich diet enhances L-cell density in obese subjects and in mice through improved L-cell differentiation. Journal of Nutritional Science, 4.
4. Asnicar, M., Köster, A., Heiman, M., Tinsley, F., Smith, D., Galbreath, E., Fox, N., Ma, Y., Blum, W. and Hsiung, H. (2002). Vasoactive Intestinal Polypeptide/Pituitary Adenylate Cyclase-Activating Peptide Receptor 2 Deficiency in Mice Results in Growth Retardation and Increased Basal Metabolic Rate. Endocrinology, 143(10), pp.3994-4006.
5. Bechtold, D., Brown, T., Luckman, S. and Piggins, H. (2007). Metabolic rhythm abnormalities in mice lacking VIP-VPAC2 signaling. AJP: Regulatory, Integrative and Comparative Physiology, 294(2), pp.R344-R351.
6. Berthoud, HR. (2002). Multiple neural systems controlling food intake and body weight. Neuroscience and Biobehavioral Reviews, 26, pp.393-428.
7. Chakraborty, T., Donthireddy, L., Adhikary, D. and Chakraborty, S. (2016). Long-Term High Fat Diet Has a Profound Effect on Body Weight, Hormone Levels, and Estrous Cycle in Mice. Medical Science Monitor, 22, pp.1601-1608.

8. Fabricius, D., Karacay, B., Shutt, D., Leverich, W., Schafer, B., Takle, E., Thedens, D., Khanna, G., Raikwar, S., Yang, B., et al. (2011). Characterization of Intestinal and Pancreatic Dysfunction in VPAC1-Null Mutant Mouse. Pancreas, 40(6), pp.861-871.
9. Farmer, S. (2005). Regulation of PPARγ activity during adipogenesis. International Journal of Obesity, 29, pp.S13-S16.
10. Feng, S., Reuss, L. and Wang, Y. (2016). Potential of Natural Products in the Inhibition of Adipogenesis through Regulation of PPARγ Expression and/or Its Transcriptional Activity. Molecules, 21(10), p.1278.
11. François, M., Barde, S., Legrand, R., Lucas, N., Azhar S., El Dhaybi, M., Guerin, C., Hökfelt, T., Déchelotte, P., Coëffler, M., et al. (2016). High-fat diet increases ghrelin-expressing cells in stomach, contributing to obesity. Nutrition, 32(6), pp.709-15.
12. Gao, H., Mejhert, N., Fretz, JA., Arner, E., Lorente-Cebrián, S., Ehrlund, A., Dahlman-Wright, K., Gong, X., Strömblad, S., Douagi, I., et al. (2014). Early B cell factor 1 regulates adipocyte morphology and lipolysis in white adipose tissue. Cell Metab., 9(6), pp.981-92.
13. Geneontology.org. (2017). GO Slim and Subset Guide | Gene Ontology Consortium. [online] Available at: http://www.geneontology.org/page/go-slim-and-subset-guide [Accessed 7 Jul. 2017].
14. Ghourab, S., Beale, K., Semjonous, N., Simpson, K., Martin, N., Ghatei, M., Bloom, S. and Smith, K. (2011). Intracerebroventricular administration of vasoactive intestinal peptide inhibits food intake. Regulatory Peptides, 172(1-3), pp.8-15.

15. Griffin, MJ., Zhou, Y., Kang, S., Zhang, X., Mikkelsen, TS., Rosen, ED. (2013). Early B-cell factor-1 (EBF1) is a key regulator of metabolic and inflammatory signaling pathways in mature adipocytes. J Biol Chem., 288(50), pp.35925-39. 3.

16. Grimaldi, B., Bellet, MM., Katada, S., Astarita, G., Hirayama, J., Armin, RH., Granneman, JG., Piomelli, D., Leff, T., et al. (2010). PER2 controls lipid metabolism by direct regulation of PPARγ. Cell Metab.,12(5), pp.509-20. 14. 3.

17. Harmar, A., Fahrenkrug, J., Gozes, I., Laburthe, M., May, V., Pisegna, J., Vaudry, D., Vaudry, H., Waschek, J. and Said, S. (2012). Pharmacology and functions of receptors for vasoactive intestinal peptide and pituitary adenylate cyclase-activating polypeptide: IUPHAR Review 1. British Journal of Pharmacology, 166(1), pp.4-17.

18. He, W., Barak, Y., Hevener, A., Olson, P., Liao, D., Le, J., Nelson, M., Ong, E., Olefsky, J. and Evans, R. (2003). Adipose-specific peroxisome proliferator-activated receptor knockout causes insulin resistance in fat and liver but not in muscle. Proceedings of the National Academy of Sciences, 100(26), pp.15712-15717.

19. Hill, J., Glazner, G., Lee, S., Gozes, I., Gressens, P. and Brenneman, D. (1999). Vasoactive Intestinal Peptide Regulates Embryonic Growth Through the Action of Activity-dependent Neurotrophic Factor. Annals of the New York Academy of Sciences, 897(1 NEUROPEPTIDES), pp.92-100.

20. Hu, E., Tontonoz, P., Spiegelman, BM. (1995). Transdifferentiation of myoblasts by the adipogenic transcription factors PPAR gamma and C/EBP alpha. Proc Natl Acad Sci U S A, 92 (21), pp.9856-9860.

21. Jozsa, R., Nemeth, J., Tamas, A., Hollosy, T., Lubics, A., Jakab, B., Olah, A., Lengvari, I., Arimura, A., Reglödi, D. (2006). Short-Term Fasting Differentially Alters PACAP and

VIP Levels in the Brains of Rat and Chicken. Annals of the New York Academy of Sciences, 1070(1), pp.354-358.

22. Kahn, B. and Flier, J. (2000). Obesity and insulin resistance. Journal of Clinical Investigation, 106(4), pp.473-481.

23. Kiehn, J., Tsang, A., Heyde, I., Leinweber, B., Kolbe, I., Leliavski, A. and Oster, H. (2017). Circadian Rhythms in Adipose Tissue Physiology. Comprehensive Physiology, pp.383-427.

24. Klemm, D., Leitner, J., Watson, P., Nesterova, A., Reusch, J., Goalstone, M. and Draznin, B. (2001). Insulin-induced Adipocyte Differentiation. Journal of Biological Chemistry, 276(30), pp.28430-28435.

25. Kousteni, S. (2012). FoxO1, the Transcriptional Chief of Staff of Energy Metabolism. Bone. 50(2), pp.437–443.

26. Laakso, M., Kuusisto, J., Stančáková, A., Kuulasmaa, T., Pajukanta, P., Lusis, A., Collins, F., Mohlke, K. and Boehnke, M. (2017). The Metabolic Syndrome in Men study: a resource for studies of metabolic and cardiovascular diseases. Journal of Lipid Research, 58(3), pp.481-493.

27. Laburthe, M., Couvineau, A., Marie, JC. (2002). VPAC receptors for VIP and PACAP. Recept Channels, 8(3-4), pp.137-53.

28. Lam, KS. (1991). Vasoactive intestinal peptide in the hypothalamus and pituitary. Neuroendocrinology, 53(Suppl 1), pp.45–51.

29. Langfelder, P. and Horvath, S. (2008). WGCNA: an R package for weighted correlation network analysis. BMC Bioinformatics, 9(1), p.559.

30. Larsson, H. and Ahrén, B. (2000). Glucose intolerance is predicted by low insulin secretion and high glucagon secretion: outcome of a prospective study in postmenopausal Caucasian women. Diabetologia, 43(2), pp.194-202.

31. Li, X. (2013). SIRT1 and energy metabolism. Acta Biochim Biophys Sin (Shanghai), 45(1), pp.51-60.

32. Li, J., Darlak, K., Southerland, L., Hossain, M., Jaye, D., Josephson, C., Rosenthal, H. and Waller, E. (2013). VIPhyb, an Antagonist of Vasoactive Intestinal Peptide Receptor, Enhances Cellular Antiviral Immunity in Murine Cytomegalovirus Infected Mice. PLoS ONE, 8(5), p.e63381.

33. Liu, R., Li, N., Lin, Y., Wang, M., Peng, Y., Lewi, K. and Wang, Q. (2016). Glucagon Like Peptide-1 Promotes Adipocyte Differentiation via the Wnt4 Mediated Sequestering of Beta-Catenin. PLOS ONE, 11(8), p.e0160212.

34. Liu, Y., Guo, Y., Zhang, L., Pei, Y., Yu, N., Yu, P., Papasian, C. and Deng, H. (2010). Biological Pathway-Based Genome-Wide Association Analysis Identified the Vasoactive Intestinal Peptide (VIP) Pathway Important for Obesity. Obesity, 18(12), pp.2339-2346.

35. Longo, KA., Charoenthongtrakul, S., Giuliana, DJ., Govek, EK., McDonagh, T., Qi, Y., DiStefano, PS., Geddes, BJ. (2008). Improved insulin sensitivity and metabolic flexibility in ghrelin receptor knockout mice. Regul Pept, 150, pp.55–61 1.

36. Loh, DH., Kuljis, DA., Azuma, L., Wu, Y., Truong, D., Wang, HB., Colwell, CS, et al. (2014). Disrupted reproduction, estrous cycle, and circadian rhythms in female mice deficient in vasoactive intestinal peptide. J Biol Rhythms, 29(5), pp.355-69.

37. MacDougald, OA., Mandrup, S. (2002). Adipogenesis: forces that tip the scales. Trends Endocrinol Metab, 13(1), pp.5–11.

38. Mori, T., Sakaue, H., Iguchi, H., Gomi, H., Okada, Y., Takashima, Y., Nakamura, K., Nakamura, T., Yamauchi, T., Kubota, N., et al. (2005). Role of Krüppel-like Factor 15 (KLF15) in Transcriptional Regulation of Adipogenesis. Journal of Biological Chemistry, 280(13), pp.12867-12875.

39. Matsuda, K., Maruyama, K., Nakamachi, T., Miura, T., Uchiyama, M., Shioda, S. (2005). Inhibitory effects of pituitary adenylate cyclase-activating polypeptide (PACAP) and vasoactive intestinal peptide (VIP) on food intake in the goldfish, Carassius auratus. Peptides, 26, pp.1611–1616.

40. Mota de sá, P., Richard, AJ., Hang, H., Stephens, JM. (2017). Transcriptional Regulation of Adipogenesis. Compr Physiol., 7(2), pp.635-674.

41. Nussdorfer, GG., Malendowicz, LK. (1998). Role of VIP, PACAP, and related peptides in the regulation of the hypothalamo-pituitary-adrenal axis. Peptides, 19, pp.1443–1467.

42. Olszewski, P., Wirth, M., Shaw, T., Grace, M. and Levine, A. (2003). Effect of peptide histidine isoleucine on consummatory behavior in rats. American Journal of Physiology - Regulatory, Integrative and Comparative Physiology, 284(6), pp.R1445-R1453.

43. Repa, J. (2000). Regulation of mouse sterol regulatory element-binding protein-1c gene (SREBP-1c) by oxysterol receptors, LXRalpha and LXRbeta. Genes & Development, 14(22), pp.2819-2830.

44. Reusch, J., Colton, L. and Klemm, D. (2000). CREB Activation Induces Adipogenesis in 3T3-L1 Cells. Molecular and Cellular Biology, 20(3), pp.1008-1020.

45. Rosen, ED., MacDougald, OA. (2006). Adipocyte differentiation from the inside out. Nat Rev Mol Cell Biol., 7(12), pp.885–896.

46. Sangiao-Alvarellos, S., Vazquez, MJ., Varela, L., Nogueiras, R., Saha, AK., Cordido, F., Lopez, M., Dieguez, C. (2009). Central ghrelin regulates peripheral lipid metabolism in a growth hormone-independent fashion. Endocrinology, 150, pp.4562–4574.

47. Schmittgen, TD., Livak, KJ. (2008). Analyzing real-time PCR data by the comparative C(T) method. Nat Protoc., 3(6), pp.1101-1108.

48. Shi, YC., Hämmerle, CM., Lee, IC., Turner, N., Nguyen, AD., Riepler, SJ., Lin, S., Sainsbury, Amanda., Herzog, H., Zhang, L. (2012). Adult-onset PYY overexpression in mice reduces food intake and increases lipogenic capacity. Neuropeptides, 46(4), pp.173-182.

49. Shimba, S., Ishii, N., Ohta, Y., Ohno, T., Watabe, Y., Hayashi, M., Wada, T., Aoyagi, T. and Tezuka, M. (2005). Brain and muscle Arnt-like protein-1 (BMAL1), a component of the molecular clock, regulates adipogenesis. Proceedings of the National Academy of Sciences, 102(34), pp.12071-12076.

50. Steffensen, KR., Schuster, GU., Parini, P., Holter, E., Sadek, CM., Cassel, T., Eskild, W., Gustafsson, J. (2002). Different regulation of the LXRalpha promoter activity by isoforms of CCAAT/enhancer-binding proteins. Biochem Biophys Res Commun., 293(5), pp.1333-1340.

51. Tachibana, T., Saito, S., Tomonaga, S., Takagi, T., Saito, ES., Boswell, T., Furuse, M. (2003). Intracerebroventricular injection of vasoactive intestinal peptide and pituitary adenylate cyclase-activating polypeptide inhibits feeding in chicks. Neurosci Lett., 339, pp.203–206.

52. Theander-Carrillo, C., Wiedmer, P., Cettour-Rose, P., Nogueiras, R., Perez-Tilve, D., Pfluger, P., Castaneda, TR., Muzzin, P., Schurmann, A., Szanto, I., et al. (2006). Ghrelin action in the brain controls adipocyte metabolism. J Clin Invest., 116, pp.1983–1993.

53. Tontonoz, P., Hu, E., Graves, RA., Budavari, AI., Spiegelman, BM. (1994). mPPAR gamma 2: Tissue-speci c regulator of an adipocyte enhancer. Genes Dev., 8, pp.1224-1234.

54. Usdin, T., Bonner, T. and Mezey, E. (1994). Two receptors for vasoactive intestinal polypeptide with similar specificity and complementary distributions. Endocrinology, 135(6), pp.2662-2680.

55. Viscarra, J., Wang, Y., Hong, I. and Sul, H. (2017). Transcriptional activation of lipogenesis by insulin requires phosphorylation of MED17 by CK2. Science Signaling, 10(467), p.eaai8596.

56. Vosko, AM., Schroeder, A., Loh, DH., Colwell, CS. (2007). Vasoactive intestinal peptide and the mammalian circadian system. Gen Comp Endocrinol., 152, pp.165–175.

57. Vu, J., Larauche, M., Flores, M., Luong, L., Norris, J., Oh, S., Liang, L., Waschek, J., Pisegna, J. and Germano, P. (2015). Regulation of Appetite, Body Composition, and Metabolic Hormones by Vasoactive Intestinal Polypeptide (VIP). Journal of Molecular Neuroscience, 56(2), pp.377-387.

58. Williams, G., Harrold, J. and Cutler, D. (2000). The hypothalamus and the regulation of energy homeostasis: lifting the lid on a black box. Proceedings of the Nutrition Society, 59(03), pp.385-396.

59. Winzell, MS., Ahrén, B. (2007). G-protein-coupled receptors and islet function-implications for treatment of type 2 diabetes. Pharmacol Ther., 116(3), pp.437-448.

60. Zhang, Y., Yin, L. and Hillgartner, F. (2000). Thyroid Hormone Stimulates Acetyl-CoA Carboxylase-α Transcription in Hepatocytes by Modulating the Composition of Nuclear Receptor Complexes Bound to a Thyroid Hormone Response Element. Journal of Biological Chemistry, 276(2), pp.974-983.

61. Zhang, L., Nguyen, A., Lee, I., Yulyaningsih, E., Riepler, S., Stehrer, B., Enriquez, R., Lin, S., Shi, Y., Baldock, P., Sainsbury, A. and Herzog, H. (2012). NPY modulates PYY function in the regulation of energy balance and glucose homeostasis. Diabetes, Obesity and Metabolism, 14(8), pp.727-736.

62. Zhou, Y., Song, T., Peng, J., Zhou, Z., Wei, H., Zhou, R., Jiang, S. and Peng, J. (2016). SIRT1 suppresses adipogenesis by activating Wnt/β-catenin signaling in vivo and in vitro. Oncotarget, 7(47), pp.77707-77720.